Interface optical phonons in spheroidal dots: Raman selection rules

F. Comas,* C. Trallero-Giner,* Nelson Studart, and G. E. Marques
Departamento de Fisica, Universidade Federal de São Carlos, 13565-905, São Carlos, SP, Brazil
(Received 9 October 2001; published 18 January 2002)

The contribution of interface phonons to first-order Raman scattering in nanocrystals with nonspherical geometry is analyzed. Interface optical phonons in the spheroidal geometry are discussed and the corresponding Fröhlich-like electron-phonon interaction is reported in the framework of the dielectric continuum approach. It is shown that the interface phonon modes are strongly dependent on the nanocrystal geometry, particularly on the ellipsoid's semiaxis ratio. The new Raman selection rules have revealed that solely interface phonon modes with even angular momentum are allowed to contribute to the first-order phonon-assisted scattering of light. On this basis we are able to give an explanation for the observed low-frequency ''shoulders'' present in the Raman cross section of several II-VI semiconductor nanostructures.

DOI: 10.1103/PhysRevB.65.073303 PACS number(s): 73.22.−f, 73.63.Kv, 71.38.−k

By using microluminescence and micro-Raman measurements, nanocrystallites or quantum dots (QD's) may be studied at an almost individual level.[1–4] QD's built from different semiconductor materials (CdSe, CdTe, PbS, CdS, etc.), embedded in a glass matrix, were intensively discussed in the later years and the spherical geometry was extensively applied, particularly for the consideration of polar-optical phonons.[5–9] In most of the quoted papers an investigation of the electron-phonon coupling was also made. The theoretical results have been compared with experimental findings; in particular, resonant Raman measurements were considered and the corresponding spectra for the first-order process show some structures on the low-frequency side of the principal peak (see, for instance, Fig. 8 of Ref. 5). The same kind of structure in the Raman line shape was also analyzed in Ref. 9, where a more realistic approach to the polar-optical phonons was applied.[7,8] As is shown in Fig. 1 these shoulders move to lower energies as the quantum dot radius decreases. It has been claimed that the ''shoulder'' on the left of the main Raman peak is due to surface-optical- (SO-) phonon-assisted transitions. However, it can be proved that, for a purely spherical geometry, such transitions are forbidden by selection rules.[7,10] In order to explain the appearance of the SO modes, the relaxation of the angular momentum $l=0$ phonon selection is invoked. The SO mode can be observed in the Raman scattering processes due to (a) impurity or interface imperfections, (b) valence band mixing, and (c) nonspherical geometry of the QD's. For this reason, the motivation of the present paper is to study the QD's geometrical shape deviation from the strictly spherical geometry and its contribution to the Raman measurements. In recent works, the electronic energy levels and wave functions of spheroidal QD's were examined.[11] In the current report we consider the polar-optical vibrations of a QD with spheroidal geometry by applying the dielectric continuum approach. We study the changes introduced in the SO-phonon eigenfrequencies, eigenstates, and also the electron-phonon Hamiltonian due to nonspherical geometry. The key point is to analyzing the selection rules for the first-order phonon-assisted Raman scattering as a function of the QD geometry. The conclusion that solely SO phonons with even angular momentum are allowed to have a contribution to the Raman spectra provides us with a strong basis for an explanation of the origin of the shoulders already invoked in previous works.

Let us briefly summarize the essential theory that we have applied. The main macroscopic quantities involved in the description of polar-optical vibrations, in particular the involved electric potential φ, is derived from the equation $\epsilon(\omega)\nabla^2\varphi=0$, where the frequency-dependent dielectric function is given by $\epsilon(\omega)=\epsilon_\infty(\omega^2-\omega_L^2)/\omega^2-\omega_T^2)$. The latter formula is valid when the phonon wavelength $\lambda_p>L$, where L is the dot dimension. Otherwise, if $\lambda_p\leqslant L$, we are in the presence of confined phonons and mixed modes involving electromechanical coupled fields should be taken into account. In this case, the interface phonon dispersion relation of the simpleminded electrostatic model can be obtained in the form of the envelope of anticrossing modes.[12] For the SO phonons $\epsilon(\omega)\neq 0$ thus, the solution of the Laplace equation,

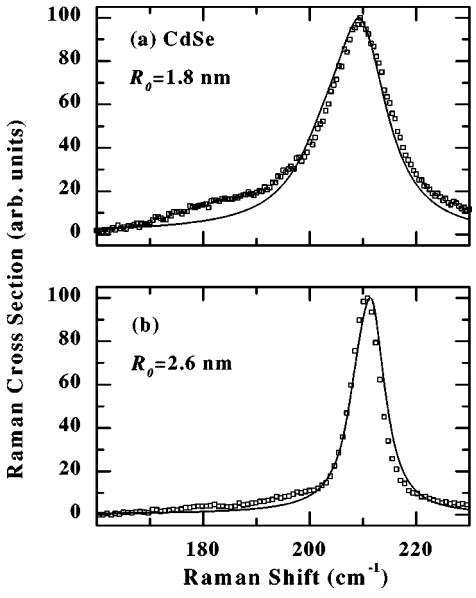

FIG. 1. First-order Raman line shape for CdSe nanocrystal from Ref. 9. (a) Mean radius $R_0=1.8$ nm. (b) Mean radius $R_0=2.6$ nm. The solid lines correspond to the calculation of the Raman spectrum assuming a QD with spherical geometry. Dots represent the spectra measurement.

φ, (i) should be continuous at the interface between two different media and (ii) must fulfill the boundary condition $\epsilon_1[\partial\varphi_1/\partial n]_S=\epsilon_2[\partial\varphi_2/\partial n]_S$. By considering a prolate spheroidal QD, the coordinates ξ,η, and ϕ are the most convenient and related to the rectangular Cartesian coordinates through the equations[13,14] $x=b\sqrt{(\xi^2-1)(1-\eta^2)}\cos\phi$, $y=b\sqrt{(\xi^2-1)(1-\eta^2)}\sin\phi$, and $z=b\xi\eta$. We also have $\xi\geqslant 1$, $-1\leqslant\eta\leqslant 1$ and $0\leqslant\phi\leqslant 2\pi$. The equation $\xi=$const describes an ellipsoid of revolution where the z direction is taken along the ellipsoid's major axis with $2b$ being the interfocal distance. For $1\leqslant\xi\leqslant\xi_0$ we have, in the ellipsoid's interior region, a semiconductor of the CdSe prototype with a dielectric function $\epsilon(\omega)$. For $\xi\geqslant\xi_0$ we shall consider a glass matrix with frequency-independent dielectric constant ϵ_D. The Laplace equation is separable in the spheroidal prolate coordinates and the solutions are given by[13]

$$\varphi^{<}=A_{lm}R_l^m(\xi)Y_{lm}(\eta,\phi),\quad \text{for}\quad \xi\leqslant\xi_0,$$
$$\varphi^{>}=A_{lm}[R_l^m(\xi_0)/Q_l^m(\xi_0)]Q_l^m(\xi)Y_{lm}(\eta,\phi),\quad \text{for}\quad \xi\geqslant\xi_0. \tag{1}$$

Notice that the potential is already continuous at $\xi=\xi_0$. The other boundary condition is fulfilled by taking $\epsilon_1\equiv\epsilon(\omega)$ and $\epsilon_2\equiv\epsilon_D$, which leads to the following result:

$$\frac{\epsilon(\omega)}{\epsilon_D}=\left(\frac{d}{d\xi}\ln Q_l^m\Big|_{\xi_0}\right)\left(\frac{d}{d\xi}\ln R_l^m\Big|_{\xi_0}\right)^{-1}\equiv f_{lm}(\xi_0), \tag{2}$$

where the functions R_{lm} and Q_{lm} are defined below. The functions $f_{lm}(\xi_0)$ are dependent on the nature neither of the constituent materials nor of the normalization of the functions R_{lm} and Q_{lm}. They do depend on the QD geometrical shape through the parameter ξ_0. The SO-phonon eigenfrequencies in the spheroidal QD are then given by

$$\frac{\omega_{lm}^2}{\omega_T^2}=\frac{\epsilon_0-\epsilon_D f_{lm}(\xi_0)}{\epsilon_\infty-\epsilon_D f_{lm}(\xi_0)}. \tag{3}$$

It is easy to show that the limit $\xi_0\to\infty$ in Eq. (3) leads to the corresponding eigenfrequencies of a purely spherical QD.[5]

The functions $R_l^m(\xi)$ and $Q_l^m(\xi)$ are defined in Ref. 13 and we shall give them here in terms of hypergeometric functions

$$R_l^m(\xi)=\frac{(2l)!(\xi^2-1)^{m/2}\xi^{l-m}}{2^l l!(l-m)!}F\left[\frac{m-l}{2},\frac{m-l+1}{2},\frac{1}{2}-l,\frac{1}{\xi^2}\right],$$

$$Q_l^m(\xi)=\frac{2^m(l-m)!\Gamma(1/2)(\xi^2-1)^{m/2}}{\Gamma(l+3/2)(2\xi)^{l+m+1}}\times F\left[\frac{l+m+1}{2},\frac{l+m+2}{2},l+\frac{3}{2},\frac{1}{\xi^2}\right]. \tag{4}$$

The functions $Y_{lm}(\eta,\phi)$ are the usual spherical harmonics and, in all cases, the quantum numbers are given by $l=1,2,3,\ldots$ and $|m|\leqslant l$. The other limit properties are that (i) $R_l^m(\xi)$ is divergent as ξ^l when $\xi\to\infty$ and are convergent at $\xi=1$; (ii) $Q_l^m(\xi)$ converges to zero as ξ^{-l-1} when $\xi\to\infty$ and diverges logarithmically at $\xi=1$. We assume $\xi_0>1$.

The corresponding electron-phonon Hamiltonian $\hat{H}_{e\text{-}ph}(\boldsymbol{r})=-e\hat{\varphi}(\boldsymbol{r})$ can be derived by standard procedures. The potential operator $\hat{\varphi}$ can be written as

$$\hat{\varphi}(\boldsymbol{r})=\sum_{lm}\frac{\epsilon_\infty\omega_L}{\epsilon_\infty-\epsilon_D f_{lm}(\xi_0)}\left[\frac{2\pi\hbar}{\epsilon^* b\,\omega_{lm}g_{lm}(\xi_0)}\right]^{1/2}\times\{F_l^m(\xi)Y_{lm}(\eta,\phi)\hat{a}_{lm}+\text{H.c.}\}, \tag{5}$$

where $F_l^m=R_l^m(\xi)$ for $\xi\leqslant\xi_0$ and $F_l^m=[R_l^m(\xi_0)/Q_l^m(\xi_0)]Q_l^m(\xi)$ for $\xi\geqslant\xi_0$. Moreover, $1/\epsilon^*=(1/\epsilon_0-1/\epsilon_\infty)$.

Let us consider the case of a CdSe spheroidal QD embedded in a glass matrix. The applied physical parameters are $\omega_T=165.2\ \text{cm}^{-1}$, $\epsilon_0=9.53$, and $\epsilon_\infty=5.72$, while for the host material, we take $\epsilon_D=4.64$.[9] For prolate ellipsoidal geometry the phonon frequencies ω_{lm} as a function of the deviation parameter ξ_0 are presented in Fig. 2(a), for $l=1,2$. Each involved SO-phonon mode is explicitly indicated in the fig-

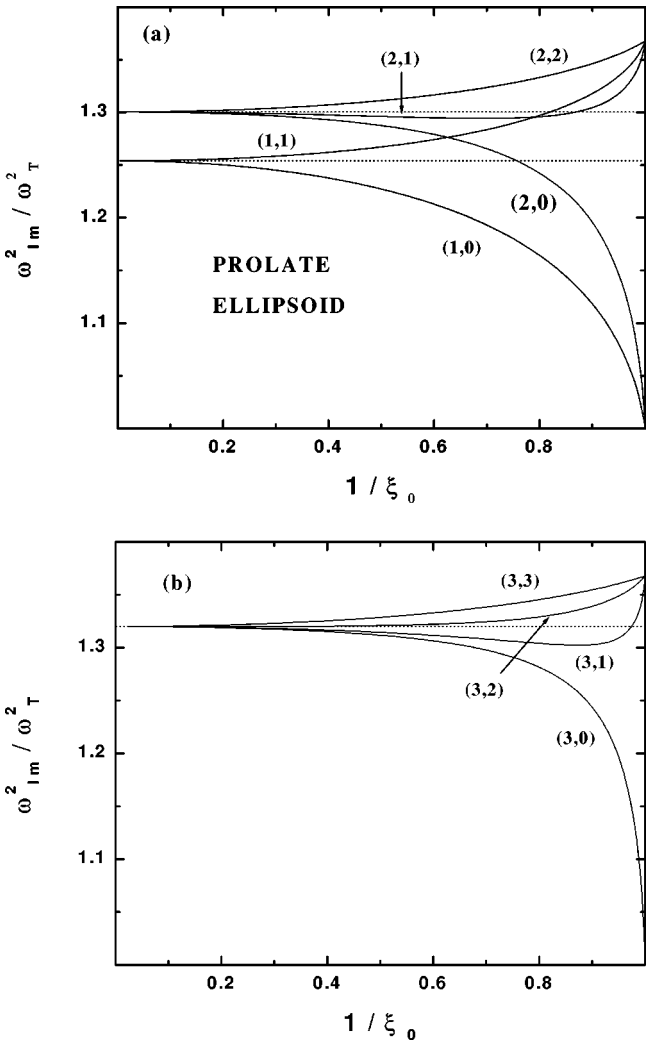

FIG. 2. (a) The squared frequencies ω_{lm}^2 in units of ω_T^2 as a function of $1/\xi_0$ for $l=1,2$ and all possible values of m for the prolate ellipsoid. (b) Same plot for $l=3$ and all possible values of m. In both cases the dotted lines correspond to the strictly spherical case.

ure. The dotted lines are the corresponding eigenfrequencies for the strictly spherical case. In Fig. 2(b) we are showing the same dependences for $l=3$. Notice the splitting of the frequencies (according to the rule $m \leqslant l$) and the main conclusion is that the separation between *SO-phonon frequencies depends on the QD dimensions* (through ξ_0). We have found that the observed frequency splitting is in the range of the structural features seen in the spectral line shapes of Fig. 1. For higher values of l we obtain lower values for the frequency splitting. Another important quantity is the ellipsoid's semiaxis ratio $r=\xi_0/\sqrt{\xi_0^2-1}$. According to Ref. 15 we should expect a ratio $1.1 \leqslant r \leqslant 1.3$. A direct comparison between the experimental data and the results here presented should provide a much better understanding of the role played by the QD geometry.

First-order resonant Raman scattering cross sections of a single QD are proportional to the square of the scattering amplitude, W_{FI}, between the initial and final states, I and F, as given by

$$W_{FI}=\sum_{\mu_1,\mu_2}\frac{\langle F|H^{+}_{E-R}|\mu_2\rangle\langle\mu_2|H_{E-P}|\mu_1\rangle\langle\mu_1|H^{-}_{E-R}|I\rangle}{(\hbar\omega_s-E\mu_2)(\hbar\omega_l-E\mu_1)}. \tag{6}$$

Here, $\omega_l(\omega_s)$ is the incoming (scattered) and $H_{E\text{-}P}(H_{E\text{-}R})$ is the electron-hole phonon (electron-radiation) Hamiltonian interaction. The corresponding electron-hole wave functions $|\mu\rangle$ were taken in the same spirit of Ref. 11, but extended to the QD exterior region; i.e., hard wall boundary conditions on the spheroid's surface were not assumed. By introducing Eq. (5) into Eq. (6) we were able to obtain selection rules for the electron-phonon transitions, which are summarized as follows: (a) Only SO phonons with $m=0$ and $l=$ even integer are allowed. Notice that $l=1$ is not allowed for the transitions in contradiction to the assumptions of previous works.[9] (b) For the electronic states (denoted as in Ref. 11) the angular momenta l_e and l_h should have the same parity, while $m_e=m_h=m$. By $e(h)$ we mean electron (hole) quantum numbers. The latter results permit us to give an interpretation for the shoulder at the left side of the main Raman peak seen in Fig. 1 as a direct consequence of the spheroidal geometry of the dot. On the other hand, the observed Raman data, together with the spheroidal SO phonons here reported, can be used in order to determine the ellipsoid's semiaxis ratio r. On the basis of data taken from Ref. 9, we have that, for the QD of Fig. 1(a) where the shoulder maximum is seen at approximately 183 cm^{-1}, the corresponding SO-phonon frequency for the prolate QD (setting $l=2$ and $m=0$) gives a ratio $r=1.86$. This result indicates that this QD has a very strong deviation from the spherical geometry. On the other hand, the shoulder maximum at 188 cm^{-1} in Fig. 1(b) with mean radius of 2.6 nm will lead to $r=1.065$, an indication that this is a sample with a shape closer to spherical geometry. The latter results confirm the general idea that QD's with large mean radius should display a more spherical shape.

We acknowledge financial support from Fundação de Amparo à Pesquisa do Estado de São Paulo (FAPESP) and Conselho Nacional de Desenvolvimento Científico e Tecnológico (CNPq). F.C. and C.T.G. are grateful to Departamento de Física, Universidade Federal de São Carlos, for hospitality.

*Permanent address: Departamento de Física Teórica, Universidad de la Habana, Vedado 10400, Havana, Cuba.

[1] A. Ekimov, J. Lumin. **70**, 1 (1996).
[2] D. Bertram, Phys. Rev. B **57**, 4265 (1998).
[3] S.A. Empedocles, D.J. Norris, and M.G. Bawendi, Phys. Rev. Lett. **77**, 3877 (1996).
[4] D.J. Norris, A. Sacra, C.B. Murray, and M.G. Bawendi, Phys. Rev. Lett. **72**, 2612 (1994).
[5] M.C. Klein, H. Hache, D. Ricard, and C. Flytzanis, Phys. Rev. B **42**, 11 123 (1990).
[6] S. Nomura and T. Kobayashi, Phys. Rev. B **45**, 1305 (1992).
[7] E. Roca, C. Trallero-Giner, and M. Cardona, Phys. Rev. B **49**, 13 704 (1994).
[8] M.P. Chamberlain, C. Trallero-Giner, and M. Cardona, Phys. Rev. B **51**, 1680 (1995).
[9] C. Trallero-Giner, A. Debernardi, M. Cardona, E. Menendez-Proupin, and A.I. Ekimov, Phys. Rev. B **57**, 4664 (1998).
[10] E. Duval, Phys. Rev. B **46**, 5795 (1992).
[11] G. Cantele, D. Ninno, and G. Iadonisi, J. Phys.: Condens. Matter **12**, 9019 (2000) and references therein.
[12] F. Comas, R. Pérez-Alvarez, C. Trallero-Giner, and M. Cardona, Superlattices Microstruct. **14**, 95 (1993).
[13] P. M. Morse and H. Feshbach, *Methods of Theoretical Physics* (McGraw-Hill, New York, 1953).
[14] *Handbook of Mathematical Functions*, edited by M. Abramowitz and I. Stegun (Dover, New York, 1972), p. 751.
[15] N. Nirmal, D.J. Norris, M. Kuno, M.G. Bawendi, Al.L. Efros, and M. Rosen, Phys. Rev. Lett. **75**, 3728 (1995).